Prairie Provinces Vulnerability Assessment for Future Climate Scenarios

Introduction:

Drought is a major cause for concern related to future climate variability. In the past, drought has been linked to costly disasters both here in western North America and throughout the world (Keyentash, 2002). Drought can be defined as a period of prolonged dry weather for a longer than a normal period, representing climate variability (Bonsal and Wheaton, 2005). There are four categories: (1) meteorological drought relates to the length of time without any measurable precipitation; (2) agricultural drought can occur if meteorological droughts persist long enough or occur at a vulnerable period in the growing season and effect soil moisture conditions; (3) hydrological drought occurs if sustained periods of no precipitation effect occurs and declines in surface or groundwater; (4) socioeconomic drought relates to the supply and demand of economic good related to extreme droughts (Heim, 2002). A meteorological drought can suddenly end but effects may persist for days/months and possibly years before the natural system recovers fully. It is important to measure and identify droughts on a regional basis rather than at a specific location for this widespread effect. Many drought-monitoring programs are in place throughout the world to understand how climate change will impact the occurrence and duration of drought. These initiatives monitor the relationship between precipitation, temperature and potential evaportranspiration and the overall impact on soil moisture and surface water (Keyantash and Dracup, 2002). Examples of drought indices include Palmer Drought Severity (Hydrological) Index (PDSI/PDHI), Climate Moisture Index (CMI) and the Standardized Precipitation Index (SPI) (Heim, 2002).

Most future climate scenarios are derived using General Circulation Models (GCM's) to assess regional vulnerability and to implement adaptation strategies. The development of biophysical impact scenarios allows for an interpretation of the potential impacts of climate change on the ecosystems, soil landscapes and water resources within Alberta and the Prairie Provinces. These ecosystems support a range of economic sectors including agriculture and forestry management practices. The impacts of climate change associated with increased greenhouse gases (GHG), projected increases in temperature and changes to precipitation influxes will influence the type of crops grown and influence forest growth rates and fire regimes. Biophysical systems react to the short-term departures from the normal climate temperature and precipitation conditions (variability) and extreme events rather than the trends in the mean climate conditions associated with climate change (Sauchyn et al., 2002).

Most future climate scenarios derived from GCM's are expressed in terms of percent change in precipitation and change in temperature degrees relative to some baseline (e.g. 1961-1990). These climate change scenarios simulate mean conditions for some future 30-year time slice (e.g. 2010-2039, i.e. the 2020's) and with less uncertainty inter-annual and seasonal variability. Since droughts are not a mean changes in climate conditions, we are interested in simulating and better understanding the extremes and variability associated with climate change scenarios. Under increased CO2 scenarios most GCMs forecast increases in winter precipitation and an overall increase in annual temperature for the Canadian Prairies. This departure of precipitation patterns and accumulation from normal conditions combined with increased temperatures may result in less summer soil water available for this region. Developing future drought

management strategies to deal with effects on soil erosion, biophysical, economic and social impacts requires a good understanding of the past and future climate variability and trends.

Assessing future climate conditions can best be put into context when compared to past climate conditions identifying changes in variability and trends. The longest instrumental climate record for the Prairies begins in the late 1800's with many beginning much more recently than this; therefore paleoclimatic records can extend the climate records back hundreds of years to develop this better understanding of past climate variability and trends. Trees are excellent proxies for reconstructing historical annual and seasonal climate moisture indices, since they require both water and heat to grow. These paleoclimatic reconstructions are useful tools for assessing the ability the GCM pre-industrial control experiments to accurately simulate past climate variability and trends.

Climate change scenarios allows for the assessment of potential impacts to water resources, aquatic and terrestrial ecosystems and soil landscapes. We can then assess the vulnerability of the economic and social sectors associated with these potential impacts to our natural resources. A good indicator of aridity is the climate moisture index (CMI), a monthly measurement of precipitation minus potential evaportranspiration.

This paper compares the annual instrumental and reconstructed CMI to historical and future scenarios of CMI from the CGCM3 (Canadian Climate Model Third Generation GCM) for the Prairie Provinces. In this analysis instrumental and proxy climate data records will be used to as analogs to assess future climate change variability and trends. Many of the methods in this paper were adapted from Burke et al. (2006) where they observed PDSI trends and variability worldwide.

Data and Methods:

The study area for this vulnerability assessment is Alberta, Saskatchewan and Manitoba – the Prairie Provinces. The annual climate variability is calculated using the climate moisture index (CMI): total monthly precipitation minus monthly potential evapotranspiration (P-PET) in cm. Hogg (1994) was able to reproduce the present distribution of vegetation for the Prairie Provinces using the same CMI of P-PET for the 1951-1980 period using the Jenson-Haise and simplified Penman-Monteith methods for calculating PET. For this analysis the Thornthwaite (1948) method was used to estimate annual PET since very few station have recorded solar radiation and wind data. The Thornthwaite PET is based on the relationship between potential evaportranspiration, temperature and shortwave radiation (number of sunlight hours per month). Little input data are required, only monthly mean temperature and total precipitation; other methods require solar radiation and wind data. The Thornthwaite formula is:

$PET=1.6(T/I)^{a}$
PET= potential evaportranspiration (cm/month), T= monthly mean air temp (C),
$a=0.49 + 0.0179\ I - 7.71 \times 10^{-5}\ I^{2} + 6.75 \times 10^{-7}\ I^{3}$
I=annual heat index
$I=\text{sum}\ (i=1:12)\ (Ti/5)^{1.5}$

Monthly historical observed precipitation and temperature data, interpolated to a 50 km grid, were taken from the Canadian Climate Archive. Further information regarding this gridded climate data is available at www.cics.uvic.ca/climate/data.htm. Climate data are sparse in the entire Prairie Provinces beginning in the late 1880's,

particularly in northern unpopulated locations. An extensive record only since 1950 is available. Therefore this project focused on 1950-1999 for complete spatial coverage. CMI was calculated at each grid point for August to July, which is a more meaningful 12-month period for vegetation than the calendar year.

Future climate and past climate simulations of CMI were obtained from the Canadian Climate Third Generation Model (CGCM3.1) with a transient resolution of 63 (www.cccma.ec.gc.ca). The T63 version has a surface spatial resolution of roughly 2.8^{o} latitude/longitude and 31 vertical levels. The Intergovernmental Panel on Climate Change (IPCC, 2007) recommends that more than one GCM and an ensemble of experiments be used to derive future climate scenarios to give a range of changes for key climate variables; for this analysis three experiments from CGCM3.1 are used. Two experiments are also used to assess the GCMs ability to simulate past climate trends and variability: (1) pre-industrial control (PIC) experiment (350 yrs: 1850-2199) has the GHG, sulfur aerosols and solar forcing agents fixed at levels of the year 1850 (CO2 = 290 ppmv, CH4 = 792 ppbv, N2O = 285 ppbv, solar constant = 1366.0 W/m^2, and sulfate aerosol from natural source); (2) 20th Century (20CM) experiment starts with atmosphere conditions comparative to start of the Industrial Revolution (1850) and runs to the year 2000. Three future scenarios are derived from SRES (Special Report on Emission Scenarios) A1b, A2 and B1 experiments for the years 2001-2100. The PIC simulation is used as a reference to the historical 20CM and SRES experiments and also provides the initial states for the 20CM (IPCC). The SRES experiments are driven by world population growth, economic growth and technology advances each effecting the atmosphere composition and in turn different effects on the future climate. As stated by

the CCCMA (www.cccma.ec.gc.ca) 'grid box values are not directly comparable to station data'. Climate models only attempt to represent the full climate system. The IPCC recommends that a regional approach, be used with no less than several grid cells, to overcome the individual grid cell biases, particularly with precipitation. For this analysis the average of nine grid cells (3x3) was used to derive a new value for the center grid cell; this 'mask' was applied to 33 grid cells representing the Prairie Provinces.

For direct comparison, the observed gridded 1950-1999 CMI 50 km was interpolated to match CGCM3.1 grid resolution of 2.8 degrees. Scenarios of future CMI were generated by applying differences in temperature and precipitation, between baseline and future periods, to observed data for the same baseline period. For example, precipitation scenarios are derived by taking the ratio of the mean value (e.g. monthly or annual) future time period (e.g. 2020's) to the baseline (e.g. 1961-99) and adjusting the observed baseline period (1961-90) by this ratio. Temperature scenarios are derived by taking the difference in mean values and adjusting the observed record. This method reduces the spatial biases in the GCMs. Scenarios of future climate change were applied to the interpolated observed P-PET values for 1961-1990 to produce maps of future aridity for three time periods: 2020's (2010-3029), 2050's (2040-2069) and 2080's (2070-2099).

The observed data set for the entire Prairie Provinces begins in 1950 although data are available for the southern region back to 1895; this however can be extended further using proxy data such as tree rings. At dry sites, trees respond to seasonal and annual precipitation and temperatures particularly winter snow accumulation and spring/early summer precipitation. At cool sites, they respond to higher temperatures.

Annual CMI was calculated for the August to July growing year is a more meaningful annual period for trees than the calendar year. Sites were sampled where soil moisture is the limiting growth factor; on open slopes facing south-to-south west. Standardized tree-ring width chronologies for Lodgepole Pine (*Pinus contorta*) from the Cypress Hills, were used to derive high-resolution annual P-PET indices at Medicine Hat, extending the instrumental record from 1895 back to 1723 (Figure 1). The reconstruction of the annual P-PET at Medicine Hat was validated using a split-sample approach that divided the full period into two subsets of equal length (1985-1946 and 1947-1999) to test the stability of the regression model used (Table 1). The R^2 values were similar; however the reduction of error (RE) value was slightly greater for the calibration period of 1947-1999. The RE statistic measures the skill of the regression model, and is applied to independent data to measure association between the series of actual values and their estimates (Fritts, 1976).

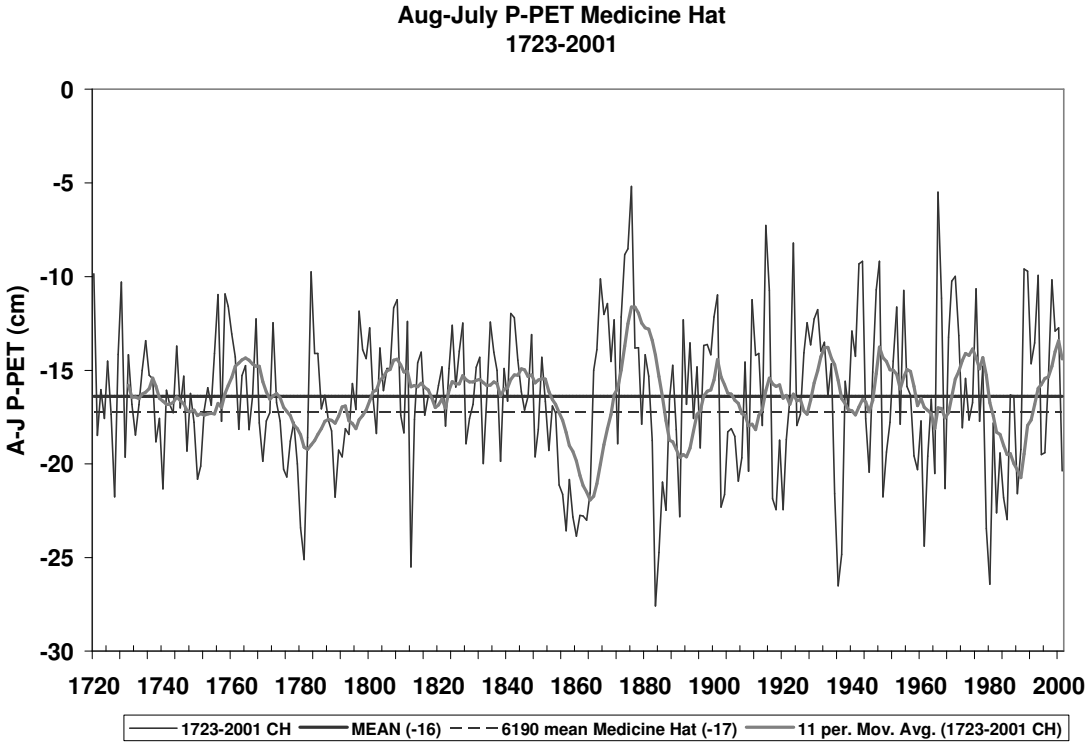

Figure 1. Reconstruction of Medicine Hat P-PET (cm) (1723-2001) from Cypress Hills standardized chronology. The solid grey line represents the 11 year moving average.

Calibration	**1895-1999**	**1895-1946**	**1947-1999**
Verification		**1947-1999**	**1895-1946**
R	0.42	0.47	**0.46**
R^2 adj	0.17	0.20	**0.20**
F	22.42	14.04	**13.99**
p-value	<0.00	<0.01	**<0.03**
SE est	10.70	10.33	**9.12**
RMSEv		12.84	**13.52**
RE		0.10	**0.14**

Table 1. Calibration and verification statistics used to reconstruct P-PET (cm) at Medicine Hat using standardized tree ring width from the Cypress Hills. (Bold values represent the statistics used in reconstruction).

Results:

Figure 2 shows average (1961-1990) P-PET (cm) conditions for the Prairie Provinces using the 50km resolution interpolated to a 10km resolution using the regularized spline method. Dry anomalies occur in the northeastern dry subhumid zone in Saskatchewan (north east of Saskatoon) and in northwestern Alberta. A CMI of -15 cm correspondences closely to the semiarid zone and the mixed grassland ecozone and -6 cm to the dry subhumid zone and the aspen parkland ecozone as seen in Figure 3.

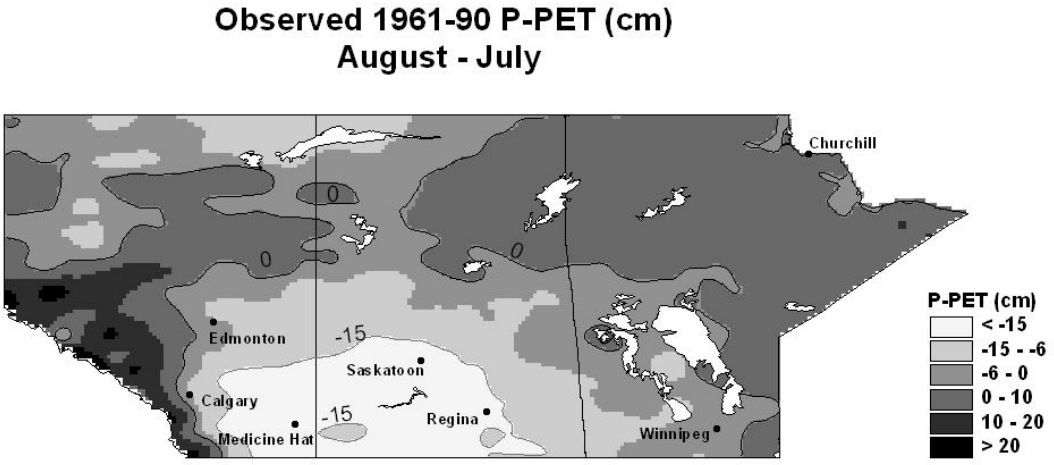

Figure 2. Average annual P-PET for the 1961-90 period, -15 cm corresponds to mixed grasslands and semi arid zone, -6 cm corresponds to aspen parkland and dry subhumid zone.

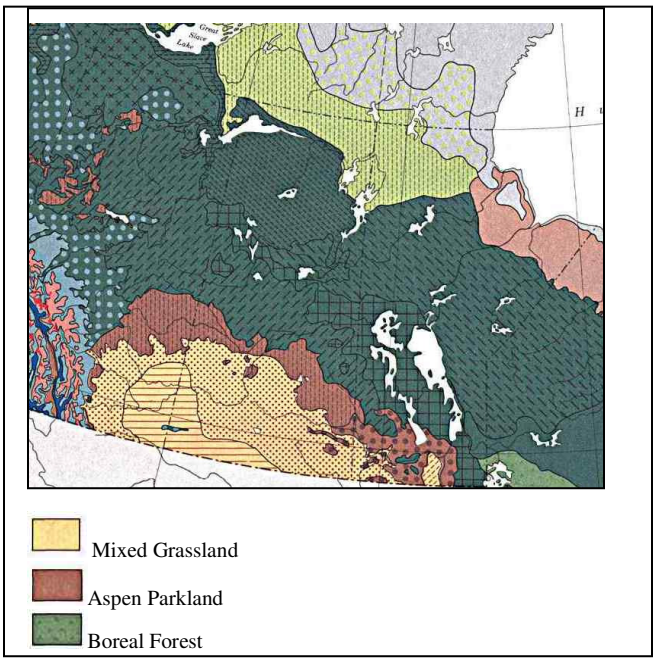

Figure 3. Vegetation zones of Canada. (National Atlas of Canada, NRC, 2007).

Verifying Pre Industrial Control Run: Tree Ring Analysis

Before any confidence can be placed in future climate scenarios from GCMs, we must validate that they can accurately reproduce the historic climate. The average P-PET value for the reconstructed Medicine Hat CMI (-16 cm) from 1723-1850 is used as the marker to define drought in the reconstruction. Percentiles do not measure the extreme drought occurrences as reconstructions the same range of variability as instrumental data, thus a specific P-PET was used to identify drought. Also, using the mean P-PET value for the entire record length and study region of the PIC as the drought marker allowed for comparison between the reconstructed and simulated aridity values (Figure 4). The entire Medicine Hat reconstructed CMI includes the pre-industrial era and the effects of increased GHG and aerosols; therefore only the period up to 1850 is comparable to the

PIC experiment. Drought durations of the CMI reconstruction range from 1 year up to 7, 9 and 11 years. The PIC simulates the longest drought to be 10 years and less at 5 and 6 year durations. Droughts were considered to be a minimal duration of 1-year. Table 2 compares the number of drought events per 100 yrs and the duration between the Medicine Hat reconstructed CMI and simulated PIC GCM experiment. The PIC experiment simulates three more drought events than the reconstruction. The average duration is similar, however the standard deviation of the reconstructed values is greater than for the PIC, suggesting that the duration of droughts has a much larger range historically than as simulated by the GCM. Overall the PIC experiment does a fair job at replicating the climate at pre-industrial conditions; however further reconstructions extending over more of the study area would be required to adequately measure the ability of the GCM. Based on this assessment the future scenarios need to be used with caution.

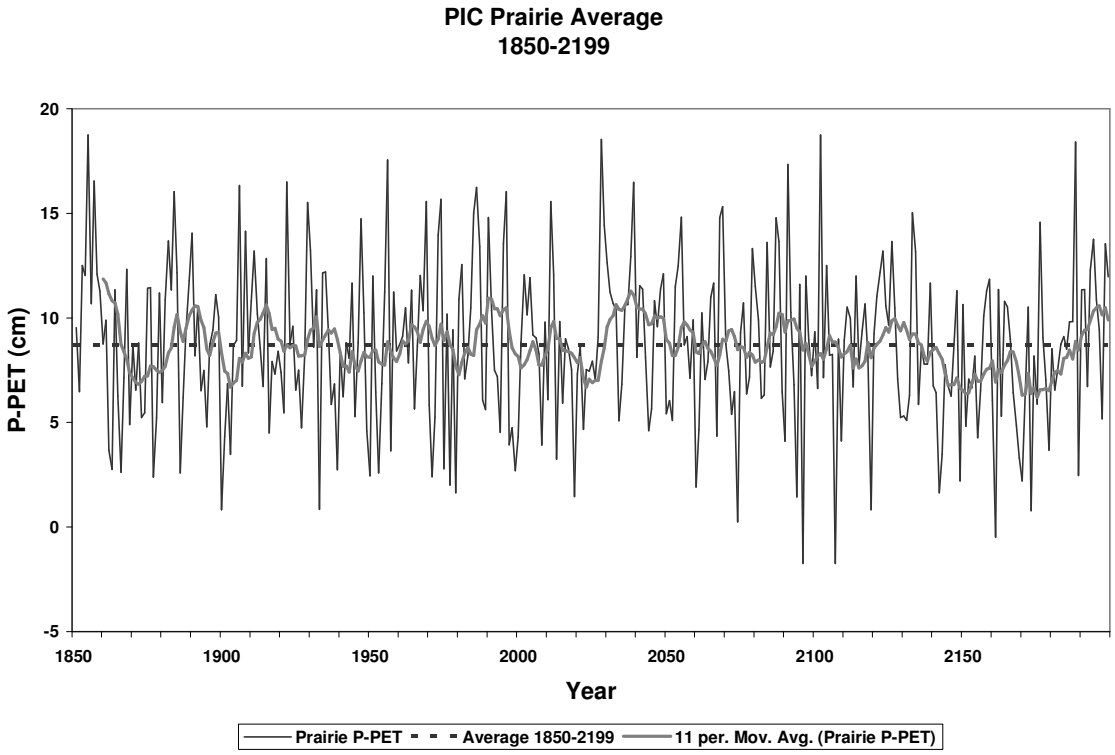

Figure 4. The average P-PET (cm) of the 33 GCM cells that cover the Prairie Provinces for the 250 year PIC scenario. The solid black line represents the mean P-PET (cm) for the entire area and period (8.7cm). The solid grey line represents the 11 year moving average.

	Recons.	PIC
# events/100yrs	19.0	22.0
Avg Duration	2.1	2.2
Std. Dev.	2.0	1.7

Table 2. Number of drought events, average drought duration and standard deviation for the reconstructed (Recons.) Medicine Hat CMI (1723-1850) and PIC (1850-2199).

20th Century Drought Conditions:

Extreme and moderate drought thresholds were identified as the 10th and 25th percentile, respectively, of the average CMI for the 1961-1990 period. That is, 10% and 25% of the entire region is under drought conditions at any time during the 1961-1990 time period. The values of -15 cm and -6 cm correspond to the 10th and 25th percentile of the observed CMI, respectively. Comparing the observed percentiles directly with the GCM values underestimated the number of droughts simulated, due to the over-estimation of precipitation by the GCM; therefore percentiles were calculated from the 20CM and observed data sets individually to represent approximately the same number of droughts.

Figures 5 and 6 show the proportion of land in drought each year between 1850 and 1999 for the 20CM run and observed from 1950-99, using the 10th and 25th percentiles as drought determinants. The 1950s appear to have been the driest period covering a very large area followed by the early 1980's for both the 10th and 25th percentiles and the observed data. The 20CM experiment also simulates extended drought periods during the late 19th century into the early 20th century and again from about 1945 to 1955. Table 3 shows the trends in percentage of total area per decade above/below drought conditions comparing the 20CM and observed aridity conditions. The 20CM experiment simulates a much greater drying trend during the last few decades compared to the observed. This rapid decrease in moisture demonstrated by the GCM results from the combination of rapid increasing temperatures and different precipitation patterns (temporal and spatial) influenced by anthropogenic GHG sources. 20CM shows a large increase in the amount of land under both the 10th and 25th percentile for the 1961-1990

period relative to 1950-99. It also simulates that the droughts will become much more extreme with a greater increase in the area of land below the 10th percentile (6.4%) than the 25th percentile (5.4%). The observed drought conditions show a small increase in moisture during the 1950-99 time period below the 25th percentile compared to the 1960-99 period which shows that aridity increases by 2% more of the region per decade; however these droughts are less extreme.

The average drought duration, number of events per 100 yrs and the total number of years per century under drought conditions are compared in Table 4 between the observed and 20CM CMI. On average the 20CM experiment has more drought occurrences for both the entire record (1850-2000) and last half of the 20th century compared to the observed 1950-99 record; this is due to the simulated increase in temperatures beginning in the 1980's as noted earlier. A short instrumental record does not pick up the major drought conditions of the mid 1870's through to 1890's; therefore these results would differ if using a longer timeline.

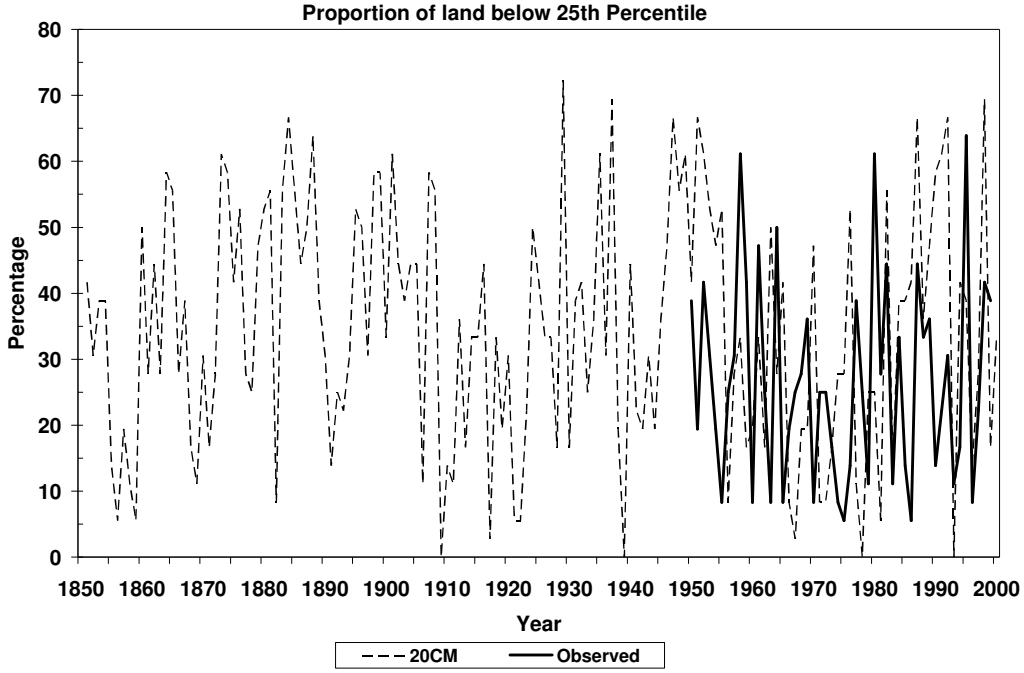

Figure 5. Time series of the total percent of the region, both for the observed and C3M P-PET annual values, below the 25th percentile of the observed and C3M 1961-1990 average P-PET.

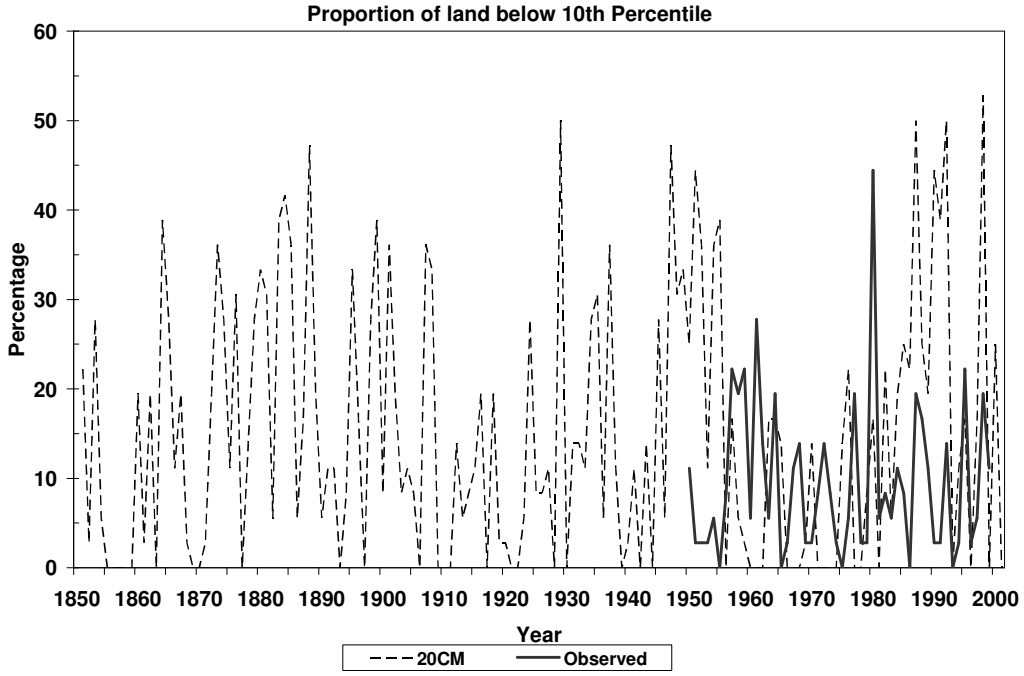

Figure 6. Time series of the total percent of the region, both for the observed and C3M P-PET annual values, below the 10th percentile of the observed and C3M 1961-1990 average P-PET.

	10th		25th	
Years	**Observed**	**20CM**	**Observed**	**20CM**
1851-1999		0.12		-0.17
1900-2000		0.62		0.10
1950-99	0.06	1.44	-0.11	0.47
1960-99	-0.20	6.40	1.95	5.42

Table 3. Percentage of increase/decrease of the land surface per decade below the 10th and 25th percentile for the observed (1950-99) and 20CM GCM run (1851-1999). Note that the amount of land increasing below the 10th percentile relative to the 25th percentile of 20CM 1950-99 is less; this suggests that the dry soil conditions are becoming less extreme relative to the overall drying.

21st Century Drought Conditions:

Three SRES experiments from the CGCM3 model also were used to simulate future aridity conditions for the region. The 10th and 25th percentiles that were calculated previously with the 20CM experiment were used as thresholds to determine the proportion of land, drought duration and number of events for the time period of 2001-2100 (Figures 7 and 8). Table 4 shows the average percentage of land for the three future periods 2020's, 2050's and 2080's for three SRES simulations below the extreme and moderate drought thresholds. The A1b experiment has a slight decrease of the land below drought conditions for the 2020's and an increase in the 2050's, this is most likely due to the increasing precipitation forecast by the GCM and then followed by a rapid increase in temperatures through the 2050's. The A1b experiment shows similar amounts of land below the 10th and 25th percentiles to those of the 20CM experiment. The A2 experiment shows the greatest increase in land under drought conditions through the 2020's and slightly decreasing in the 2050's, but still above the 61-90 average of the

20CM experiment. Rarely does the amount of land under the 25th percentile drop below 15%, which is much higher than for the 20CM. The area of land also below the 10th percentile for the region rarely reaches 0% compared to the 20CM experiment, which tends to have 0% of the total region under drought conditions nearly once every ten years. This suggests that not only does this model simulate more frequent drought but also more extreme. The experiment B1 forecasts the greatest overall increase in percentage of land below both the 10th and 25th percentile. It also simulates the most extreme events; in the late 2020's nearly 60% of the entire region is under extreme (10th) drought conditions; then a few years later none of the region is in extreme drought conditions. From the 2070's through the end of the century drought conditions improve enough only once to decrease the total area of land below extreme drought conditions to 0% of the area for the 10th percentile or below 10% of the area for the 25th percentile; much more extreme than the other two experiments (Figures 5 and 6). By the end of the 21st century on average one-third of the Prairie Provinces will be in moderate (25th) drought conditions and one-fifth below extreme drought conditions, this is double the 1961-90 extent.

These results also correspond to the average drought duration and number of events expected under future conditions for each of these SRES experiments. Table 5 compares the future and historic drought events. On average all three SRES experiments have longer drought duration (except A2 and B1 during the 2050's) and the same or decreased number of events per century (except A2 2050's) compared to the 20CM experiment. The A1b experiment shows the least increase in drought duration, number of events and total increase of land below drought conditions relative to A2 and B1 experiments for the 2080's. The A2 experiment simulates the average changes and B1

the most extreme future drought conditions. According to the B1 scenario by the end of this century drought will have increased in duration with more extreme events and cover more of the region. The A1b experiment shows a more positive outlook with slight decreases in the drought duration and events; however the overall total land below both moderate and extreme drought conditions increases.

	A1b		A2		B1	
Period	**10th**	**25th**	**10th**	**25th**	**10th**	**25th**
2020	8%	22%	15%	35%	15%	33%
2050	15%	32%	17%	33%	13%	28%
2080	13%	25%	16%	31%	21%	36%

Table 4. Average total percent of the Prairie Province region in drought conditions, below 10^{th} and 25^{th} percentile, for the three future time periods.

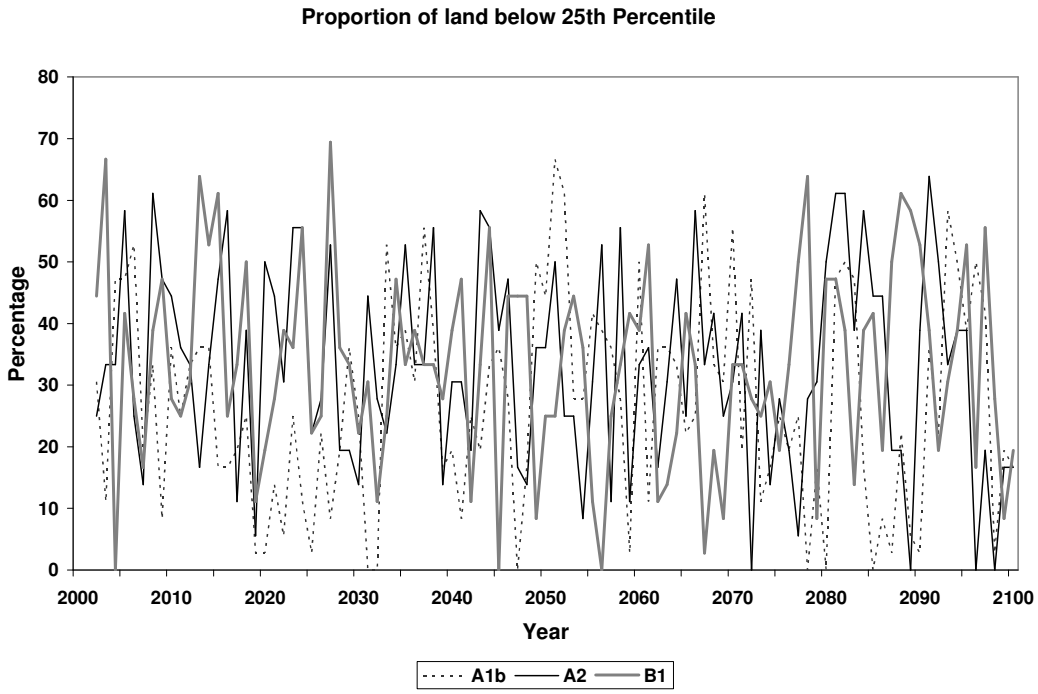

Figure 7. Total proportion of the Prairie Provinces for the future P-PET scenarios below the 1961-90 (20CM) 25th percentile.

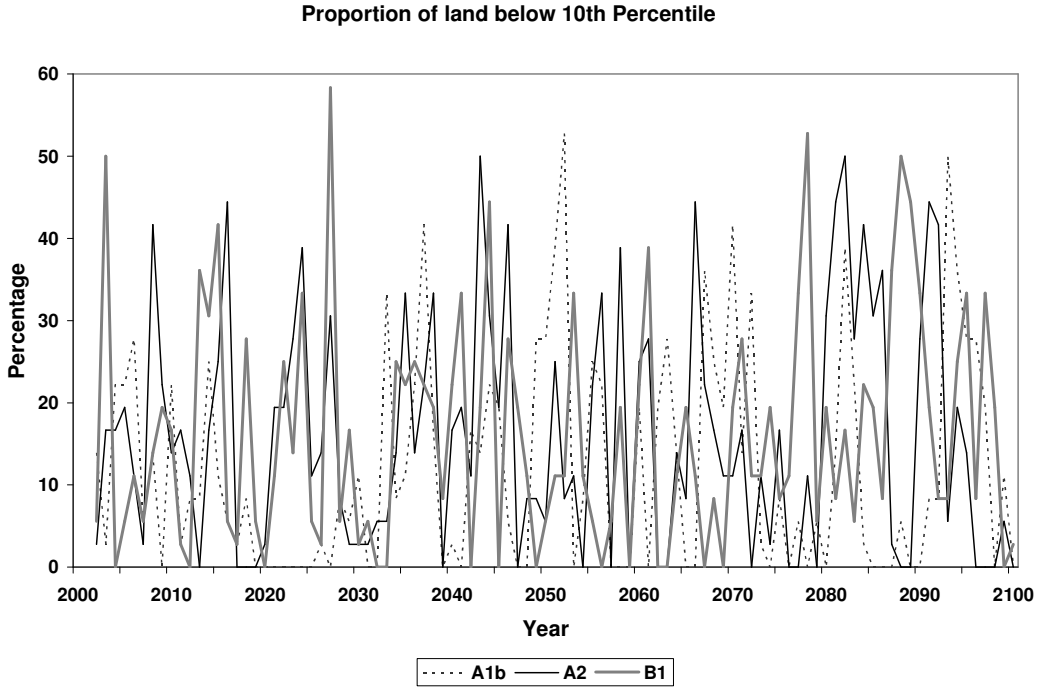

Figure 8. Total proportion of the Prairie Provinces for the future P-PET scenarios below the 1961-90 (20CM) 10th percentile.

	Observed	20CM		A1b			A2			B1		
	1950-99	1850-2000	1950-99	2020	2050	2080	2020	2050	2080	2020	2050	2080
Avg Duration yrs	1.7	1.8	1.8	2.3	2.2	1.8	2.1	1.6	2.3	1.8	1.5	2.2
Events/100 yrs	5.7	9.3	8.2	5.1	7.4	6.0	8.2	10.8	6.9	9.3	7.9	9.3
Total/100 yrs	10	16	14	12	16	11	17	18	16	16	12	21

Table 5. Comparison of the average drought duration, number of drought events and the total years (per 100 yrs) that are below the 10^{th} percentile, for the observed, 20CM, and future scenarios.

Low Frequency variability:

An 8-year low pass digital filter (Fritts, 1976) was used to smooth the annual P-PET for each of the 33 grid cells that cover the Prairie Provinces and retain information that was greater than timescales of 8-years. Empirical Orthogonal Function (EOF) and principle components (PCs) for the time scale corresponding to each EOF were used to analyze trends in the observed P-PET and 20CM and SRES P-PET experiments. The eigenvalues that correspond to the first PC and EOF capture over 85% of the observed P-PET variance and 95% of the GCM variance. The first PC and EOF represent the average P-PET for each grid cell location. Figure 9 shows the spatial patterns generated by the EOF analysis; negative (positive) values represent dry (wet) moisture conditions. Figure 10 shows the spatial distribution associated with EOF1 and displays the standardized CMI values for the region. The spatial pattern of EOF1 for observed data closely matches Figure 1, which is expected. Figure 9 shows the 20CM P-PET values for the same time (1950-99); the GCM simulates wetter conditions along the mountains and southeastern Alberta. Northern Alberta through all of Saskatchewan and Manitoba are much drier than the observed values. Overall the pattern is similar but the GCM appears to shift values to the east relative to observed values. A correlation of 0.39 was found between the observed and 20CM EOF1 values for the 1950-99 years. Figure 10a shows the PC1 for the temporal change in moisture over the Prairie Provinces; there is a strong PDO pattern evident with shifts from a negative PDO to positive PDO during the 1977-78 season (Mantua and Hare, 2002). The negative PDO pattern begins in 1947 with 1957-58 being positive PDO phases and 1969-1970 also has an increase in the PDO value (not above zero) which can be seen in the observed PC1. During negative PDO phases

the sea surface temperature is warmer in the North Pacific and cooler along the west coast of North America bringing cooler wet conditions to the Prairies (Bonsal and Lawford, 1999), the opposite pattern exists for positive PDO phases. It is interesting that the same temporal pattern is visible in the GCM as the observed data; thus the model is capturing some of the low frequency variability of the PDO cycle.

Figure 10b shows the standardized PC1 for the SRES experiments for the future conditions; natural variability is also being modeled by the GCM. There is an overall trend with a decrease in the P-PET values associated with the increase in standardized value. Higher values tend to be associated with drier conditions as seen in the observed PC1 which corresponds to the PDO cycle. Figures 9 also shows the P-PET spatial pattern for each of the SRES experiment under future conditions, A1B the most conservative and B1 the most extreme conditions.

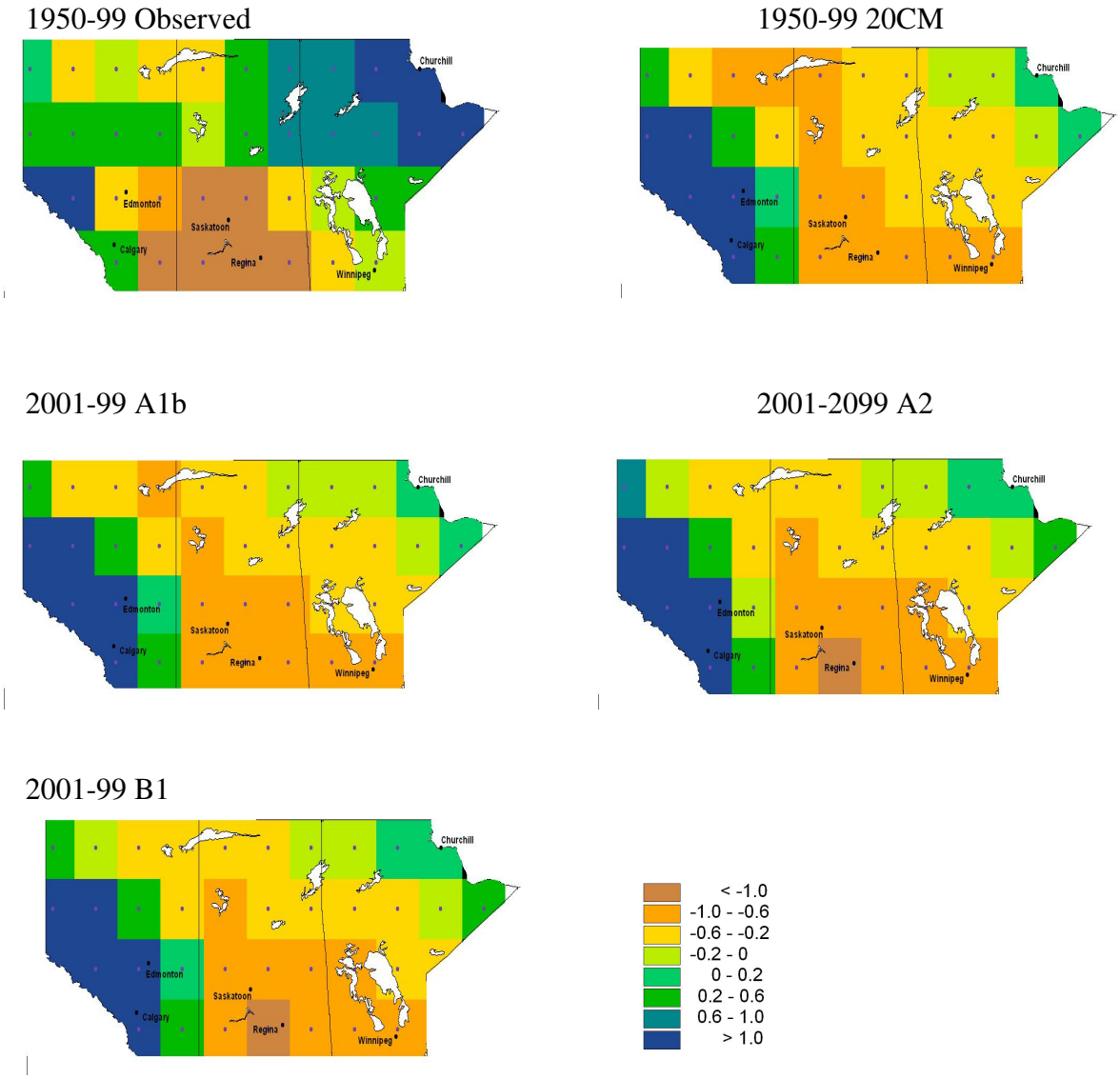

Figure 9. The spatial patterns for the first eof of the Observed (1950-99), 20CM 1950-99, and A1b, A2, B1 (2001-2100), with an 8 year low pass filter. These patterns correspond to the average P-PET (cm) values for the time period. Positive (negative) values represent high (low) soil moisture.

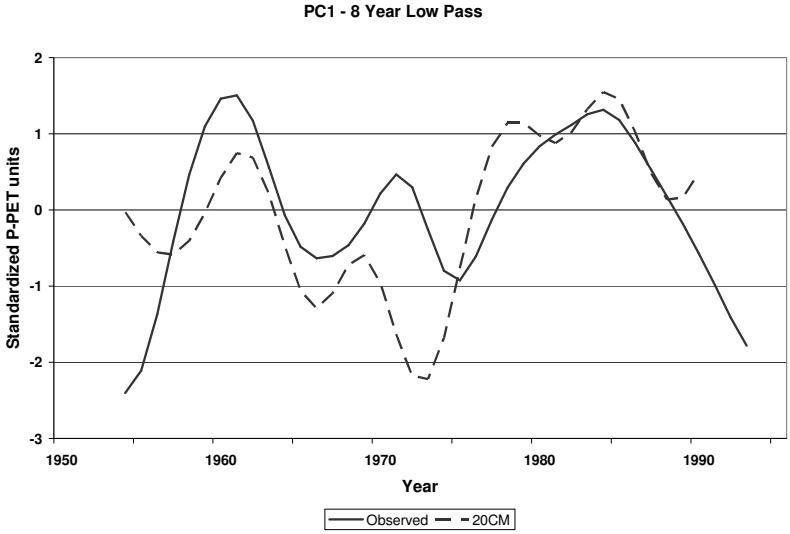

a.

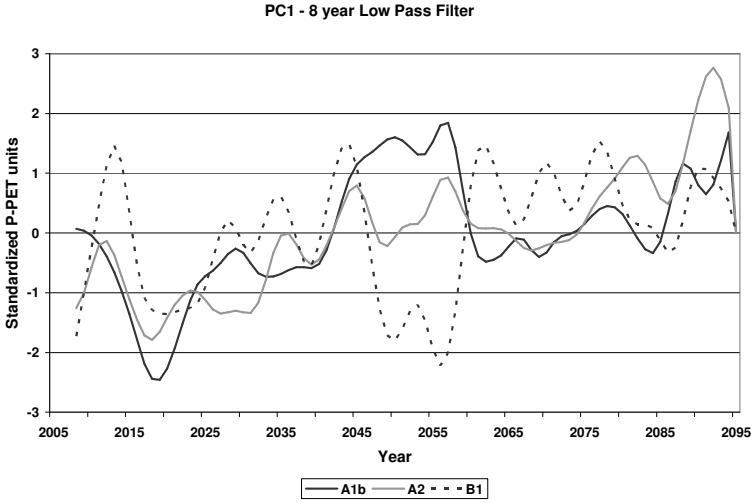

b.

Figure 10. The first principle component after filtering annual data for timescales greater than 8 years. a. Compares the observed and 20CM timescales trends. b. Compares the future scenarios. The first eigenvalue explains 86% of observed and over 95% of the GCM annual P-PET values.

Climate Scenarios:

Future P-PET climate scenarios were derived for the Prairie Provinces for three future time periods (Figure 11). The A1b scenario forecasts increased P-PET for the entire Prairie region with most increase expected in the north and along the foothills and mountain of Alberta and northeastern Manitoba. By the 2080's the semiarid region and dry subhumid regions have extended further east covering much of southern Manitoba; however the northern Prairies have become wetter (Figure 11a). Table 6 shows the change in percentage of land below the -15cm (semiarid, grassland) and -6cm (dry subhumid, aspen parkland) P-PET threshold values. Currently (1961-1990 baseline) 1900 ha are semiarid and 3900 ha are dry subhumid. The scenario of A1b by the end of this century shows an overall decrease in the amount of land in the dry subhumid zone with little change to the semiarid zone. A2 scenarios forecast (Table 6) that the greatest change will be within the next 30 years with increasing areas of both semiarid and dry subhumid conditions, extending further east and north into Manitoba (Figure 11b). Very little moisture increase is forecast along the mountain and northern region of the prairies until the 2050's through the 2080's; however this increase helps offset the increased area below the -6 cm P-PET value. B1 future scenario forecasts the most extreme drying conditions of the three SRES experiments. The climate becomes so dry that by the 2080's the semiarid region has expanded enough to encompass the Cypress Hills (SW Saskatchewan) (Figure 11c). By the 2080s, 2700 ha will be considered semi arid conditions and 4400 ha dry subhumid. The least change in moisture conditions is forecast with the A1b experiment, but in both the A2 and B1 scenarios the area known as "Pallisers Triangle" grows, expanding further north and east. Although A1b actually has

a decrease in the amount of land below both -15 cm and -6 cm, this change is reflecting the increase in precipitation for the northern prairies and along the mountains and foothills of Alberta; the arid and semi arid conditions are still expanding. Conditions forecast for the 2080's by A2 and B1 are similar to those of past drought conditions of the 'dirty thirties' and 1961 (Sauchyn et al., 2002).

a) A1b 2020

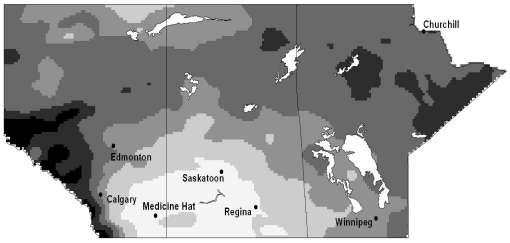

A1b 2050

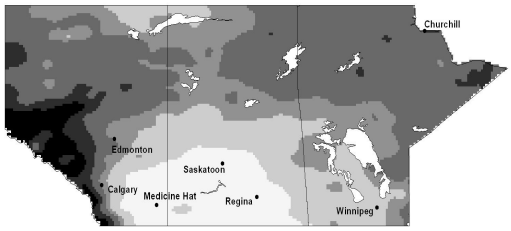

A1b 2080

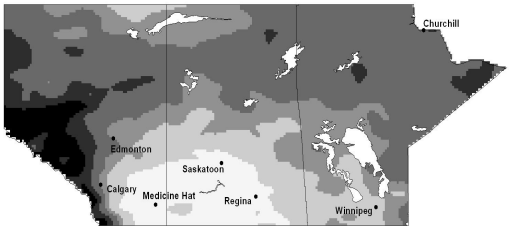

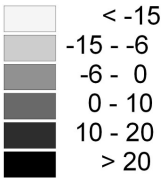

b) A2 2020

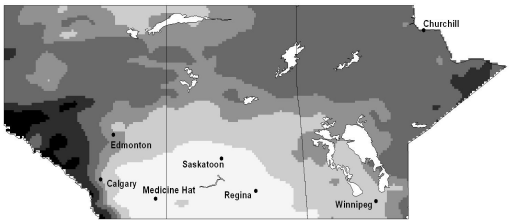

A2 2050

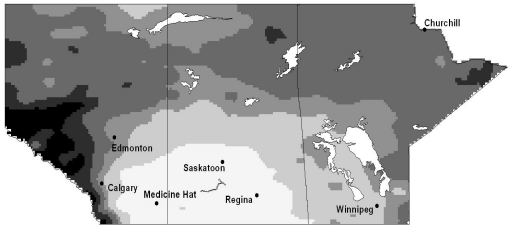

A2 2080

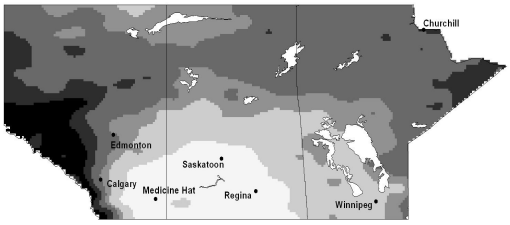

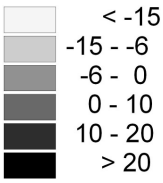

c) B1 2020 B1 2050

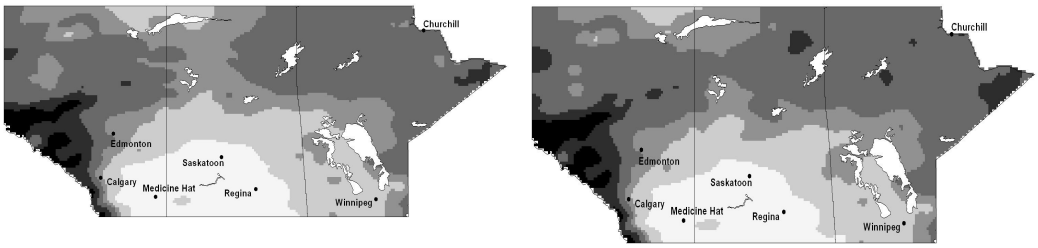

B1 2080

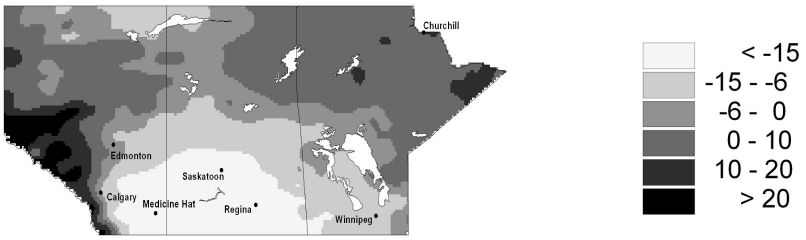

Figure 11. Forecast climate scenarios for the future time periods 2020's, 2050's and the 2080's, all relative to the observed 61-90 mean P-PET (cm) for the three SRES: (a) A1b, (b) A2 and (c) A1b.

	A1b		A2		B1	
Period	**< -15**	**< -6**	**< -15**	**< -6**	**< -15**	**< -6**
2020	-1.7	-5.3	2.5	1.7	1.8	3.0
2050	1.4	1.4	2.7	-0.2	1.1	0.2
2080	-0.3	-2.0	1.5	0.1	3.9	2.3

Table 6. Change in the total percent of land above/below the threshold values of -15 cm and -6 cm for the future climate scenarios relative to the observed 1961-90 average areas. These threshold values correspond to the 10^{th} and 25^{th} percentiles respectively, of the observed 1961-90 average P-PET values and currently define vegetation zones.

Conclusion:

This analysis is a preliminary step to investigating long-term trends and variability of future climate scenarios using the Climate Moisture Index of precipitation minus potential evapotranspiration, as modeled by the Canadian Climate Third Generation Model. Analysis was conducted for the Prairie Provinces of Canada for the years 1950 to 1999 using observed climate data and reconstructed to 1723 for Medicine Hat using standardized tree-ring chronologies from the Cypress Hills.

The standardized tree-ring chronologies were used to assess the GCMs ability to model past drought conditions. The pre-industrial control model appears to model more drought events at shorter durations than observed in the reconstructed CMI for Medicine Hat.

Drought events were measured as extreme and moderate, using the 10^{th} and 25^{th} percentiles, of the 1961-1990 CMI baseline period to compare drought events between the past climate and future climate scenarios. All three-future climate scenarios show an expanding aridity zone in the southern Prairies reaching further into Manitoba. B1 forecasts the worst-case scenario with nearly one-third of the Prairie region below the moderate aridity index by the 2080's. The duration and number of drought events remains relatively similar under the A1b scenario but duration increases for both A2 and B1 scenarios.

At timescales great than 8 years the 20^{th} Century model reproduces a similar pattern to the observed data. These patterns appear to follow the PDO signal, switching from a positive phase in 1947 to negative and again positive in 1977. This teleconnection between positive PDO phases and dry periods on the prairies has been well documented

(Bonsal and Lawford, 1999; Bonsal and Wheaton, 2005; and Mantua and Hare, 2002). Future climate variability follows a similar pattern of the observed and 20th Century but a declining trend in P-PET is evident. Using such a short instrumental record makes it difficult to detect any changes being influences by anthropogenic emissions.

In general water is being relocated from the south to the north Prairies; this will have substantial impacts on farming practices, irrigation, hydro projects and forest management practices. Further analysis using soil types needs to be considered when comparing future climate zones to current. The current semiarid and dry subhumid zones are found mainly in the brown to dark brown soil zones, which have lower water holding capacities than the black soil zones. The type of soil may buffer and slow the effects of a drying climate. Any expansion of agriculture in a new ecozone will require the assessment of the sensitivity of this landscape to both climate change and an altered vegetation cover. Other methods to calculate potential evaportranspiration should also be considered along with multiple GCMs.

Further Research:

This paper analyzes only the long-term trends and variability under future climate conditions, but it is also important to look at the inter-annual variability. I used a high-pass filter for timescales less than 8 years for the 1920-1999 southern prairies data and found a correlation value of 0.6 between SOI and PCI. Since I was doing this analysis for the entire Prairie Province region I decided to leave it out and basically ran out of time, but definitely could integrate it into this paper. I would like to build CMI reconstructions from our chronologies to derive a surface extending records further back.

This would then be used to analyze high and low frequency variability (hmmm sounds like my phd...). Also Burke et al., 2006 analyze P-PET decadal trends for each grid cell, this would also be better represented using a longer historic timescale.

References:

Bonsal, B. and E. Wheaton. 2005. Atmospheric circulation comparisons between the 2001 and 2002 and the 1961 and 1988 Canadian Prairie droughts. *Atmosphere-Ocean.* 42(2), 163-172.

Bonsal, B. and R.Lawford. 1999.Teleconnections between el-nino and la-nina events and summer extended dry spells on the Canadian Prairies. *Int. J. Climatology*. 19, 1445-1458.

Burke, E.J., Brown, S.J. and N. Christidis. 2006. Modeling the recent evolution of global drought and projections for the Twenty-First Century with the Hadley Centre Climate Model. J. of Hydrometeorology. 7(5) 1113-1125.

Diaz, H.F., Hoerling, M.P., and J.K. Eischeid. 2001. Enso Variability, Teleconnections and Climate Change. *Int. J. Climatology*. 21, 1845-1862.

Fritts, H.C., 1976. Tree rings and climate: London, Academic Press, 567 p.

Heim, R.R. Jr. 2002, A review of twentieth-century drought indices used in the United States. *American Meteorological Society (BAMS).* August, 1149-1165.

Hogg, E.H. 1994. 1997. Climate and the southern limit of the western Canadian boreal forest. *Canadian Journal of Forest Research*. 24, 1835-1845.

IPCC: Intergovernmental Panel on Climate Change, 2007.www.ipcc.ch

Keyantash, J. and J. Dracup. 2002. The Quantification of Drought: An Evaluation of Drought Indices. *American Meteorological Society (BAMS*). August, 1167-1180.

Mantua, N.J. and S.R. Hare. 2002. The Pacific Decadal Oscillation: Review. *J.of Oceanography.* 58, 35-44.

Natural Resources Canada, 2007. http://atlas.nrcan.gc.ca

Sauchyn, D.J., Barrow, E., Hopkinson, R.F., and P.R. Leavitt. 2002. Aridity on the Canadian Plains. *Geographie physique et Quaternairie*. 56(2-3), 247-259.

Thornthwaite, C.W. 1948. An approach toward a rational classification of climate. *Geogr. Rev.*, 21, 633-655.